Supramolecular Chemistry

International Edition: DOI: 10.1002/anie.201508257
German Edition: DOI: 10.1002/ange.201508257

Template-Free Synthesis of a Molecular Solomon Link by Two-Component Self-Assembly

Young Ho Song[+], Nem Singh[+], Jaehoon Jung, Hyunuk Kim, Eun-Hee Kim, Hae-Kap Cheong, Yousoo Kim, and Ki-Whan Chi**

Abstract: *A molecular Solomon link was synthesized in high yield through the template-free, coordination-driven self-assembly of a carbazole-functionalized donor and a tetracene-based dinuclear ruthenium(II) acceptor. The doubly interlocked topology was realized by a strategically chosen ligand which was capable of participating in multiple CH···π and π–π interactions, as evidenced from single-crystal X-ray analysis and computational studies. This method is the first example of a two-component self-assembly of a molecular Solomon link using a directional bonding approach. The donor alone was not responsible for the construction of the Solomon link, and was confirmed by its noncatenane self-assemblies obtained with other similar ruthenium(II) acceptors.*

The topologically intriguing threaded molecular architectures such as catenanes,[1] trefoil,[2] and pentafoil[3] knots, Solomon links (a doubly-interlocked [2]catenane),[4] and Borromean rings[5] have attracted a great deal of attention not only because of their aesthetic charm but also because of their potential applications in nanomaterials, biomaterials, molecular machines, electronic devices, and sensors.[6] Synthesis and properties of knots and links at the molecular level will certainly provide new insight to understanding these biomolecules and materials.[7,8] In this regard, ruthenium-metal-centered, coordination-driven self-assembly for the construction of discrete two- and three-dimensional supramolecular architectures has seen rapid growth in recent years.[9] These supramolecular architectures are potential materials for host–guest chemistry,[10] selective sensing,[11] and especially for drug delivery,[12] and anticancer studies.[13] The synthesis of [2]catenanes has become routine with a plethora of strategies available. However, synthesis of more topologically complex and mechanically interlocked molecular architectures such as Solomon links (SLs), pentafoil knots, and Borromean rings, is still a great challenge. Only a few examples of SLs have been prepared so far and templating approaches have been the primary methodology used in their preparations.[4] Figures 1 a–c show the previously known and common approaches for the synthesis of SLs.[4]

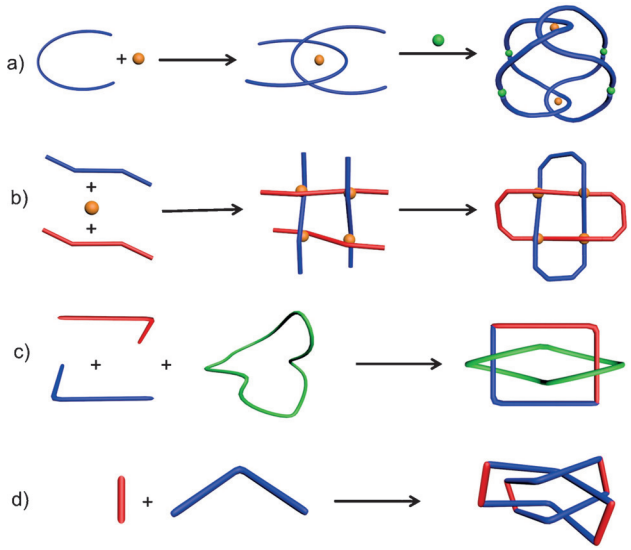

Figure 1. Methods for the synthesis of molecular Solomon links: a) metal templating followed by self-assembly, b) interwoven strategy using metal template followed by ring closing reactions, c) self-assembly using external loop, and d) two-component, coordination-driven self-assembly (this work).

We recently reported the template-free self-assembly of a molecular Hopf's link,[14] an interlocked prismatic cage,[15] and a noncatenane rectangle-in-rectangle,[16] all of which likely occur through CH···π, π–π, and other noncovalent interactions. Herein we report the one-pot synthesis of a SL through a ruthenium-directed, two-component self-assembly. The doubly entwined topology was obtained from the coordination-driven self-assembly of the arene/Ru^{II} acceptor **1** and the 3,6-di(pyridin-4-yl)carbazole donor (**5**; Scheme 1). The equimolar mixture of **1** and **5** was stirred in CD_3OD for 6 hours at room temperature and the ^1H NMR spectrum was recorded. The complex ^1H NMR spectrum indicated the quantitative formation of a new self-assembled architecture, as the α- and β-pyridyl protons were shifted by 0.1–0.8 ppm

[*] Y. H. Song,[+] Dr. N. Singh,[+] Dr. J. Jung, Prof. K.-W. Chi
Department of Chemistry, University of Ulsan
Ulsan 680-749 (Republic of Korea)
E-mail: jjung2015@ulsan.ac.kr
kwchi@ulsan.ac.kr
Dr. H. Kim
Energy Materials Laboratory, Korea Institute of Energy Research
Daejeon 305-343 (Republic of Korea)
E.-H. Kim, Dr. H.-K. Cheong
Protein Structure Group, Korea Basic Science Institute
162 Yeongudanji-Ro, Ochang, Chungbuk 28119 (Republic of Korea)
Dr. Y. Kim
Surface and Interface Science Laboratory, RIKEN
Wako, Saitama 351-0198 (Japan)
[+] These authors contributed equally to this work.

Supporting information for this article is available on the WWW under http://dx.doi.org/10.1002/anie.201508257.

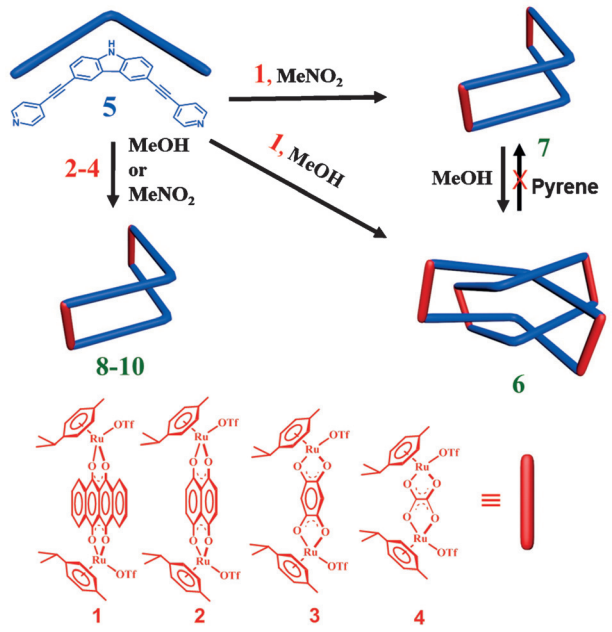

Scheme 1. Formation of the Solomon link **6** and self-assembly of the compounds **7**–**10**.

from 8.60 and 7.51 ppm, respectively. The ^{1}H NMR spectra remain the same during the course of reaction (up to 2 days). The product was then precipitated and collected, by the addition of diethyl ether, as **6**. The ^{1}H NMR spectrum of the pure product indicated a dimeric structure as all signals from **1** and **5** were significantly shifted and split into more than two kinds of signals (see Figures S1 and S2 in the Supporting Information). The NMR study clearly indicated more complex topology than for the usual [2]catenane. In the ESI-MS spectrum of **6**, the prominent signal at $m/z = 1753.0$ ($[M-3\,\mathrm{OTf}]^{3+}$ confirmed the dimeric composition (see Figure S3). The theoretical isotopic distribution was also found to be in good agreement with the experimental peaks. The collective NMR and ESI-MS data revealed the presence of a dimeric structure in solution. The doubly entwined topology of **6** was conclusively confirmed by single-crystal X-ray analysis in the solid state.

To further investigate the effect of solvent on the self-assembly, we carried out the identical reaction of **1** and **5** in CD_3NO_2 instead of CD_3OD, and it resulted in **7**. The ^{1}H NMR spectrum of the reaction mixture recorded after 6 hours was entirely different from that of **6** because the α-pyridinyl protons ($\delta = 8.53$ ppm, upfield) and β-pyridinyl protons ($\delta =$ 7.28 ppm, upfield) were significantly shifted in comparison to those of **5** (see Figures S4 and S5). DOSY, ROESY, and multinuclear NMR spectroscopy collectively confirmed that **7** has a non-interlocked structure (see Figures S7 and S9). The ESI-MS spectrum of **7** further confirmed its monomeric nature with a prominent signal at m/z 801.9 ($[M-3\,\mathrm{OTf}]^{3+}$; see Figure S6). The theoretical isotopic distribution was also in good agreement with the experimental peaks. Interestingly, upon increasing the concentration of the CD_3NO_2 solution, the interlocked structure **6** also started to form. Therefore isolation and solid-state characterization of **7** remained impossible and the structure of **7** was identified only in a dilute solution (< 4 mmol) of nitromethane.

The ROESY and DOSY NMR analyses were performed in CD_3NO_2 to compare the structures of **6** (originally prepared in methanol) and **7**. The ROESY spectrum of **6** showed multiple space-coupling interactions for almost all the neighboring protons, thus confirming a more complex interwoven structure (see Figure S8) whereas in the spectrum of **7** all the coupling interactions between neighboring protons were well-defined to indicate a simple discrete molecule (see Figure S9). The coupling interactions between the α,β-pyridyl protons and α-pyridyl-*p*-cymene protons also confirmed the coordination between the metal and ligand. The DOSY spectra of **6** and **7** (3.0 mmol in CD_3NO_2) were recorded separately at 298 K, thus providing the diffusion coefficients $D = 4.4\times10^{-10}$ and 5.4×10^{-10} m^2 s^{-1}, respectively, which confirmed their different identities (Figure 2). The DOSY

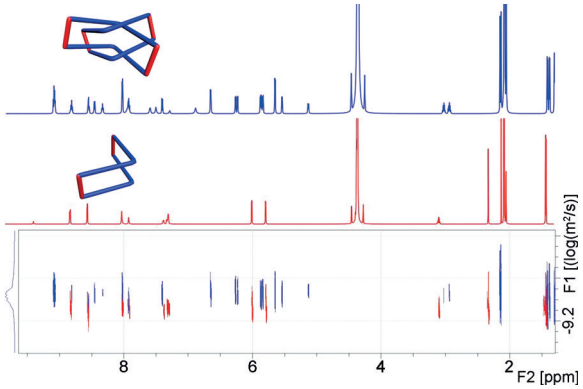

Figure 2. Comparison of DOSY NMR spectra of **6** (blue) and **7** (red) in CD_3NO_2. Assignment of signals is provided in Figures S2, S9, and S15.

spectrum of **6** at a 3.0 mmol concentration in CD_3NO_2 also confirmed that **6** is stable even in a dilute solution and not converting to **7**. Combined multinuclear and various two-dimensional NMR, ESI-MS, and elemental analyses confirmed the interlocked dimeric structure of **6** and the monomeric structure of **7** in solution (see Figures S1–S15).

The bent, rather than planar structures, of the macrocycles **7**–**10** (Scheme 1) were taken into account as per computational calculation results (see Figure S30). Their simple NMR spectra might have resulted from fast conformational rotation of ligand moieties on the NMR timescale. Comparison of the ^{1}H NMR spectra of **6** and **7** shows that the former has a doubly interlocked topology in solution, based on the following argument: The latter shows only one signal for the eight methyl groups of the isopropyl moieties, whereas the spectrum of the former shows four signals for sixteen methyl groups of the isopropyl moieties (see Figure S12). The symmetry of **6**, based on its X-ray crystal structure is D_2, each of the three C_2-symmetry axes makes just two non-equivalent isopropyl groups. The methyl groups of a given isopropyl substituent are diastereotopic, therefore is a total of four different methyl signals. If the topology of **6** were [2]catenane, its symmetry would be C_2 (lower than D_2) and

the ^{1}H NMR spectrum would be much more complex, considering the bent ligand and restricted rotation.

To investigate whether only **5** was responsible for the doubly-interlocked structure, we carried out the identical reactions using slightly different acceptors (**2**–**4**; Scheme 1), both in methanol and nitromethane solvents, to obtain the corresponding self-assembled macrocycles **8**–**10**. Multinuclear NMR and ESI-MS analyses confirmed that **8**–**10** have non-interlocked macrocycles in solution (see Figures S16–S27). The solid-state structure of **8** was also confirmed by single-crystal X-ray analysis[17] (Figure 3).

We have recently shown that an interlocked ruthenium-(II) metallacycle was reversible to a non-catenane rectangle upon addition of pyrene.[14] To investigate the template effect on the doubly interlocked dimeric structure, a methanol solution of **6** was stirred with 2.0 to 10.0 equivalents of pyrene at 25 and 60 °C while ^{1}H NMR spectra were recorded at an interval of 2 hours. No change was observed in the spectra of the reaction mixture over the course of up to 24 hours, thus confirming no effect of the π-electron-rich template on the stability of **6**. A similar self-assembly reaction of **1** and **5** in the presence of pyrene also resulted in **6**. No change was observed in the ^{1}H NMR spectra of **6** after keeping it at room temperature for several days in nitromethane.

The single-crystal X-ray analysis unambiguously confirmed the doubly interlocked topology of **6** as a SL and the non-interlocked structure of **8** (Figure 3).[17] Single crystals of **6** and **8** suitable for analysis were obtained by slow vapor diffusion of diethyl ether into their concentrated methanol/nitromethane (1:1) solution at room temperature.

The refined X-ray crystal structure of **6** shows the two macrocyclic components are doubly interlocked by the four crossings at the ethynyl bonds which define the topology of a SL. The ethynyl bonds are nearly perpendicular and the π–π stacking distances between ethynyl–ethynyl groups were found in the range of 3.48–3.86 Å. The shortest interaction in the link was found to be 3.31 Å, an interaction between ethynyl and pyridyl donor atoms, whereas the minimum distance between pyridyl-pyridyl atoms was 3.53 Å. The mean plane of pyridyl and benzene rings of the carbazole donor was almost orthogonal to the mean plane of the tetracene rings as a result of the CH···π interactions in an edge-to-face stacking pattern in the range of 2.76 to 3.47 Å. There are four such edge-to-face stacks stabilizing the SL structure as all four tetracene units are individually involved. These two factors, π–π and edge-to-face stacking are probably the driving forces behind the stability of the doubly interlocked topology. In the solid-state structure of **8**, the two identical molecules were found to be partially stacked without interlocking. The stacked structure was stabilized by parallel π–π stacking in the range of 3.43 to 3.94 Å. One of the two naphthyl rings was involved in a CH···π interaction with a carbazole unit at a distance of 2.91 Å.

A computational study was performed to gain insight into the formation of **6**, and semiempirical and density-functional theory (DFT) methods were used for geometry optimizations and binding energy (BE) evaluations, respectively (see the Supporting Information for computation details). CH···π interactions and π–π stacking were found to be the major

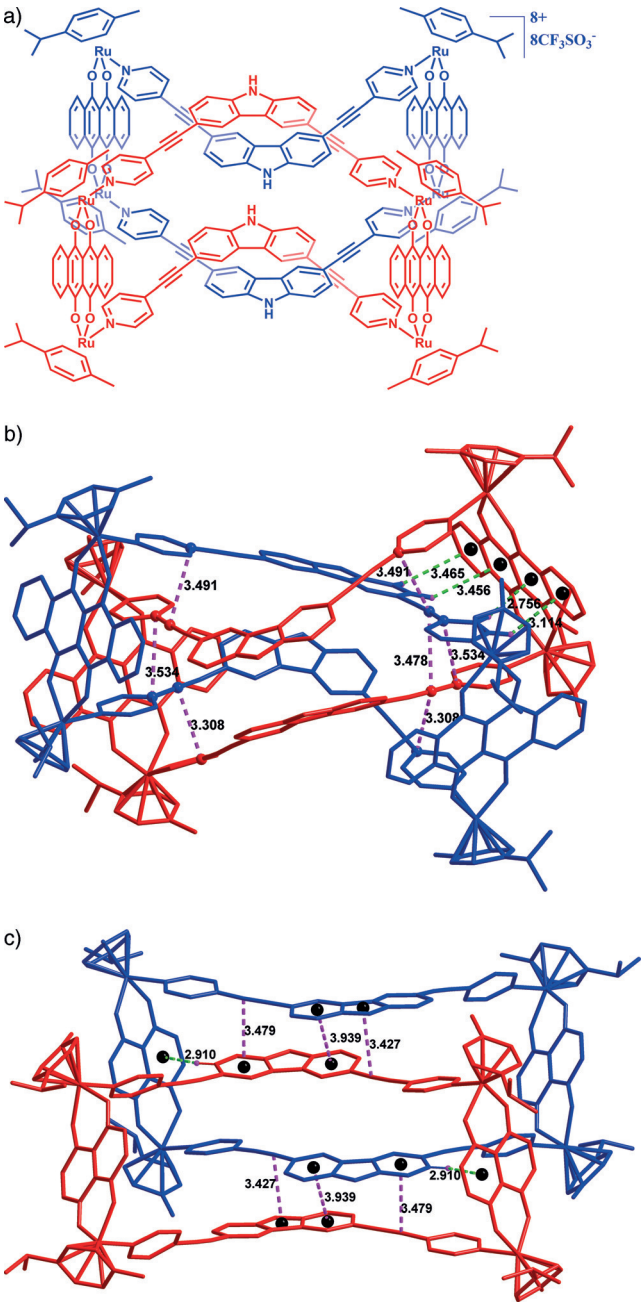

Figure 3. a) Chemical structure of **6**. X-ray crystal structures of the Solomon link **6** (b) and non-interlocked macrocycle **8** (c) in stick model showing π–π stacking (dashed pink lines) and CH···π interactions in an edge-to-face fashion (dashed green lines). Hydrogen atoms, counter ions, and solvent molecules are omitted for clarity.

intermolecular interactions, and agrees well with the geometrical characters observed by X-ray diffraction (see Figure S32). The BE for the formation of **6** from two monomers of **7** was evaluated to be −103.5 kcal mol^{-1}, which indicates that intermolecular interactions of doubly interlocked structure provide the sufficient stabilization of **6** with the carbazole unit at a distance of 2.91 Å.

Furthermore, the data in Figure 4 clearly indicates the higher thermodynamic stability, that is, larger BE, of **6** compared to three other doubly-interlocked structures simu-

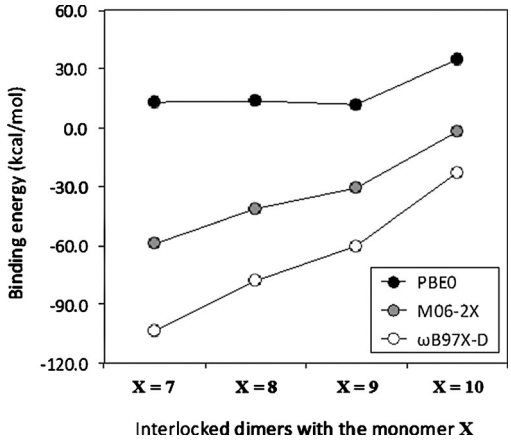

Figure 4. Calculated binding energies [*E*(doubly interlocked system)–(2×*E*(monomer))] of interlocked dimeric structures simulated with the monomer X.

lated from **8**, **9**, and **10**. Despite the structural similarity, the participation of the tetracene moiety in the intermolecular interactions provides the superior stability of **6** compared to that of the other interlocked systems. The BE differences between **6** and the doubly-interlocked system simulated with **8** are 25.6 and 17.5 kcal mol^{-1} for ωB97X-D and M06-2X, respectively (Figure 4). The additional benzene rings of the tetracene moieties, compared to naphthalene moieties, are responsible for the larger BE of **6**, and result from increased CH···π interactions. The computational results revealed the superior thermodynamic stability of **6** over the other interlocked systems simulated with **8**, **9**, and **10**, and it is mainly attributed to CH···π van der Waals interactions (see the Supporting Information for details).

In conclusion, we have successfully employed a simple, two-component self-assembly strategy using a specially equipped carbazole-functionalized pyridyl donor and a tetracene-based dinuclear ruthenium(II) acceptor for the synthesis of a molecular Solomon link in 93% yield. This ruthenium-directed self-assembly provided the Solomon link without assistance of any template. As evidenced by X-ray crystal structures, the required four crossings to form a Solomon link were provided by π–π interactions between ethynyl and pyridyl groups. The doubly interlocked structure was further stabilized by CH···π interactions, in an edge-to-face fashion, between tetracene rings and pyridyl-carbazole hydrogen atoms. Theoretical calculations also supported the stability of the Solomon link over other similar simulated doubly interlocked structures.

Acknowledgments

This work was supported by the Basic Science Research program through the National Research Foundation of Korea (2013R1A1A2006859 to K.W.C. and 2014R1A1A2007897 to N.S.). Priority Research Centers program (2009-0093818) through the NRF is also financially appreciated. H.K. thanks to Research and Development Program of KIER (B5-2513). X-ray diffraction experiments were performed at the Pohang Accelerator Laboratory. We are grateful for the use of the Hokusai-GreatWave supercomputer system of RIKEN.

Keywords: noncovalent interactions · self-assembly · structure elucidation · supramolecular chemistry · X-ray diffraction

How to cite: *Angew. Chem. Int. Ed.* **2016**, *55*, 2007–2011
Angew. Chem. **2016**, *128*, 2047–2051

[1] a) M. Fujita, *Acc. Chem. Res.* **1999**, *32*, 53; b) C. P. McArdle, M. J. Irwin, M. C. Jennings, R. J. Puddephatt, *Angew. Chem. Int. Ed.* **2007**, *46*, 218; *Angew. Chem.* **2007**, *119*, 222; c) Z. Niu, H. W. Gibson, *Chem. Rev.* **2009**, *109*, 6024; d) J. E. Beves, B. A. Blight, C. J. Campbell, D. A. Leigh, R. T. McBurney, *Angew. Chem. Int. Ed.* **2011**, *50*, 9260; *Angew. Chem.* **2011**, *123*, 9428; e) R. S. Forgan, J.-P. Sauvage, J. F. Stoddart, *Chem. Rev.* **2011**, *111*, 5434; f) G. Gil-Ramírez, D. A. Leigh, A. J. Stephens, *Angew. Chem. Int. Ed.* **2015**, *54*, 6110; *Angew. Chem.* **2015**, *127*, 6208.

[2] a) J. Guo, P. C. Mayers, G. A. Breault, C. A. Hunter, *Nat. Chem.* **2010**, *2*, 218; b) N. Ponnuswamy, F. B. L. Cougnon, J. M. Clough, G. Dan Pantos, J. K. M. Sanders, *Science* **2012**, *338*, 783; c) G. Zhang, G. Gil-Ramírez, A. Markevicius, C. Browne, I. J. Vitorica-Yrezabal, D. A. Leigh, *J. Am. Chem. Soc.* **2015**, *137*, 10434.

[3] a) J. F. Ayme, J. E. Beves, D. A. Leigh, R. T. McBurney, K. Rissanen, D. Schultz, *Nat. Chem.* **2012**, *4*, 15; b) D. A. Leigh, R. G. Pritchard, A. J. Stephens, *Nat. Chem.* **2014**, *6*, 978.

[4] a) J.-F. Nierengarten, C. O. Dietrich-Buchecker, J.-P. Sauvage, *J. Am. Chem. Soc.* **1994**, *116*, 375–376; b) F. Ibukuro, M. Fujita, K. Yamaguchi, J.-P. Sauvage, *J. Am. Chem. Soc.* **1999**, *121*, 11014; c) C. D. Pentecost, K. S. Chichak, A. J. Peters, G. W. V. Cave, S. J. Cantrill, J. F. Stoddart, *Angew. Chem. Int. Ed.* **1999**, *38*, 3376; *Angew. Chem.* **1999**, *111*, 3571; d) C. Peinador, V. Blanco, J. M. Quintela, *J. Am. Chem. Soc.* **2009**, *131*, 920; e) J. E. Beves, C. J. Campbell, D. A. Leigh, R. G. Pritchard, *Angew. Chem. Int. Ed.* **2013**, *52*, 6464; *Angew. Chem.* **2013**, *125*, 6592; f) N. Ponnuswamy, F. B. L. Cougnon, G. D. Pantoş, J. K. M. Sanders, *J. Am. Chem. Soc.* **2014**, *136*, 8243; g) C. Schouwey, J. J. Holstein, R. Scopelliti, K. O. Zhurov, K. O. Nagornov, Y. O. Tsybin, O. S. Smart, G. Bricogne, K. Severin, *Angew. Chem. Int. Ed.* **2014**, *53*, 11261; *Angew. Chem.* **2014**, *126*, 11443; h) J. E. Beves, J. J. Danon, D. A. Leigh, J.-F. Lemonnier, I. J. Vitorica-Yrezabal, *Angew. Chem. Int. Ed.* **2015**, *54*, 7555; *Angew. Chem.* **2015**, *127*, 7665.

[5] a) K. S. Chichak, S. J. Cantrill, A. R. Pease, S.-H. Chiu, G. W. V. Cave, J. L. Atwood, J. F. Stoddart, *Science* **2004**, *304*, 1308; b) S.-L. Huang, Y.-J. Lin, T. S. A. Hor, G.-X. Jin, *J. Am. Chem. Soc.* **2013**, *135*, 8125; c) S.-L. Huang, Y.-J. Lin, Z.-H. Li, G.-X. Jin, *Angew. Chem. Int. Ed.* **2014**, *53*, 11218; *Angew. Chem.* **2014**, *126*, 11400.

[6] a) C. Dietrich-Buchecker, M. C. Jimenez-Molero, V. Sartor, J. P. Sauvage, *Pure Appl. Chem.* **2003**, *75*, 1383; b) T. Ikeda, J. F. Stoddart, *Sci. Technol. Adv. Mater.* **2008**, *9*, 014104; c) E. R. Kay, D. A. Leigh, *Angew. Chem. Int. Ed.* **2015**, *54*, 10080; *Angew. Chem.* **2015**, *127*, 10218.

[7] a) W. R. Wikoff, L. Liljas, R. L. Duda, H. Tsuruta, R. W. Hendrix, J. E. Johnson, *Science* **2000**, *289*, 2129; b) J. Sakamoto, J. van Heijst, O. Lukin, A. D. Schlüter, *Angew. Chem. Int. Ed.* **2009**, *48*, 1030; *Angew. Chem.* **2009**, *121*, 1048; c) L. Hu, C. H. Lu, I. Willner, *Nano Lett.* **2015**, *15*, 2099.

[8] a) S. Saha, K. C. F. Leung, T. D. Nguyen, J. F. Stoddart, J. I. Zink, *Adv. Funct. Mater.* **2007**, *17*, 685; b) J.-F. Ayme, J. E. Beves, C. J. Campbell, D. A. Leigh, *Chem. Soc. Rev.* **2013**, *42*, 1700.

[9] a) M. Fujita, M. Tominaga, A. Hori, B. Therrien, *Acc. Chem. Res.* **2005**, *38*, 369; b) B. H. Northrop, Y.-R. Zheng, K.-W. Chi, P. J.

Stang, *Acc. Chem. Res.* **2009**, *42*, 1554; c) R. Chakrabarty, P. S. Mukherjee, P. J. Stang, *Chem. Rev.* **2011**, *111*, 6810; d) T. R. Cook, Y.-R. Zheng, P. J. Stang, *Chem. Rev.* **2013**, *113*, 734; e) T. R. Cook, P. J. Stang, *Chem. Rev.* **2015**, *115*, 7001.

[10] a) N. P. E. Barry, B. Therrien, *Eur. J. Inorg. Chem.* **2009**, 4695; b) N. P. E. Barry, J. Furrer, J. Freudenreich, G. Süss-Fink, B. Therrien, *Eur. J. Inorg. Chem.* **2010**, 725; c) N. Singh, J.-H. Jo, Y. H. Song, H. Kim, D. Kim, M. S. Lah, K.-W. Chi, *Chem. Commun.* **2015**, *51*, 4492.

[11] a) A. Mishra, S. Ravikumar, Y. Song, N. S. Prabhu, S. H. Hong, H. Kim, S. Cheon, J. Noh, K.-W. Chi, *Dalton Trans.* **2014**, *43*, 6032.

[12] a) B. Therrien, G. Süss-Fink, P. Govindaswamy, A. K. Renfrew, P. J. Dyson, *Angew. Chem. Int. Ed.* **2008**, *47*, 3773; *Angew. Chem.* **2008**, *120*, 3833; b) J. E. M. Lewis, E. L. Gavey, S. A. Cameron, J. D. Crowley, *Chem. Sci.* **2012**, *3*, 778; c) B. Therrien, *Chem. Eur. J.* **2013**, *19*, 8378.

[13] a) V. Vajpayee, Y. J. Yang, S. C. Kang, H. Kim, I. S. Kim, M. Wang, P. J. Stang, K.-W. Chi, *Chem. Commun.* **2011**, *47*, 5184; b) A. Mishra, S. C. Kang, K.-W. Chi, *Eur. J. Inorg. Chem.* **2013**, 5222; c) B. Therrien, *CrystEngComm* **2015**, *17*, 484.

[14] H. W. Lee, P. Elumalai, N. Singh, H. Kim, S. U. Lee, K.-W. Chi, *J. Am. Chem. Soc.* **2015**, *137*, 4674.

[15] A. Mishra, A. Dubey, J. W. Min, H. Kim, P. J. Stang, K.-W. Chi, *Chem. Commun.* **2014**, *50*, 7542.

[16] V. Vajpayee, Y. H. Song, T. R. Cook, H. Kim, Y. Lee, P. J. Stang, K.-W. Chi, *J. Am. Chem. Soc.* **2011**, *133*, 19646.

[17] CCDC 1421630 and 1421631 (**6** and **8**) contain the supplementary crystallographic data for this paper. These data can be obtained free of charge from The Cambridge Crystallographic Data Centre.

Received: September 7, 2015
Revised: November 19, 2015
Published online: December 28, 2015

